Journal of Environmental Analytical Chemistry

Shammala and Chiswell, J Environ Anal Chem
2018, 5:3
DOI: 10.4172/2380-2391.1000247

Research Article Open Access

Glucose-Reduced Nano-Graphene Oxide with Excellent Accumulation Removal of Pharmaceuticals and Personal Care Products from Water

Shammala FA[1*] **and Chiswell B**[2]

[1]*Department of Pharmacy, University of Palestine, El-Zahra City, Gaza, Palestine*

[2]*National Research Centre for Environmental Toxicology, University of Queensland, Brisbane, Australia*

***Corresponding author:** Shammala FA, Adjunct Professor, Department of Pharmacy, University of Palestine, El-Zahra City, Gaza, Palestine, Tel: 599-860-526; E-mail: drfaridshammala@hotmail.com

Received date: September 10, 2018; **Accepted date:** September 18, 2018; **Published date:** September 21, 2018

Abstract

Accumulation and removal of pharmaceuticals and personal care products (PPCPs) such as naproxen, ibuprofen and oxybenzone, bezafibrate, clofibric acid, carbamazepine, diclofenac from aqueous solutions was investigated using glucose-reduced nano-graphene oxide (nrGO) under UV light. Graphite oxide was firstly oxidized by nitronium ions (NO^{2+}) solution using microwave heating to get nano-GO (nGO) with about 50 nm of diameter, and then nGO was reduced in glucose at 135°C for 30 min to get nrGO with about 40 nm of diameter. The nrGO under UV light was very effective in removing pharmaceuticals, exhibits excellent accumulation and removal of diclofenac, naproxen and carbamazepine by more than 95%, while bezafibrate, ibuprofen and oxybenzone was eliminated by 80%. Clofibric acid was more stable, only eliminated by 60%. The synthesis mechanism of nrGO nanocomposite was tested and characterized with Scanning electron microscopy (SEM), Fourier transform infrared spectroscopy (FTIR), X-ray photoelectron spectroscopy (XPS), Raman spectroscopy, Atomic force microscopy (AFM) image analysis, UV-Vis spectra, X-ray diffraction patterns, thermogravimetric analysis (TGA) and Differential scanning calorimetry (DSC). The adsorption capacity of diclofenac, naproxen and carbamazepine to nrGO nanocomposite was the highest (approx. 500.0 mgg^{-1}, 493.4 mgg^{-1}, 490.5 mgg^{-1}). The calculated maximum adsorption capacities of bezafibrate, ibuprofen, oxybenzone and Clofibric acid under UV light were 325.5, 348.2, 315.8, and 245.3 mg/g, respectively).

Keywords: Graphene oxide; Nitronium oxidation; Glucose reduction; Nanocomposites; Drug; Photodegradation

Introduction

Surface and drinking water are a very valuable natural resource and its quality is essential for the survival of living creatures on the earth. However, rapid industrialization is continuously degrading the quality of water due to the addition of huge amounts of pollutants into the water bodies [1,2]. Recently, pharmaceuticals and personal care products (PPCPs) have been found in our environment, such as antibiotics, hormones, antipyretic drugs, triclosan, etc. represent a new type of pollutant in surface water; and represents a risk for both human health and environment pollution. Indeed, pharmaceuticals and personal care products (PPCPs) have been given much attention because of their huge production and necessity in human life and consumption worldwide [3]. PPCPs often persistence in the environment and are inadvertently dumped into the water bodies [4-6]. So far, various PPCPs have been found in natural surface water and even in the tissues of fishes and vegetables [7,8]. Indeed, the exact effect of PPCPs on human health and the environment is still not completely understood. Recent reports indicated that PPCPs cause several health problems, such as endocrine disruptions and change hormonal actions [9,10].

Different types of methods have been applied for the accumulation and removal of PPCPs from water, such as mesoporous material absorbents (transition metal-grafted), biodegradation, chlorination, advanced oxidation processes (AOPs) and ozonation [11-20]. These methods have disadvantages, there removal of PPCPs from water requires more improvement. For example, AOP and ozonation have not proven to be completely successful and require high energy consumption and the formation of residual byproducts [21,22]. Indeed, adsorption is an excellent method for the removal of PPCPs from the environment considering the mild operation conditions, low energy consumption, and nonexistent of side products. Moreover, Nanotechnology offers good and efficient opportunity for removing several types of pollutants present in today's wastewater by the process of adsorption. Indeed, the most widely studied adsorbents for the removal of PPCPs in literature is carbonaceous materials, including carbon nanotubes, activated carbon, and bone char [23].

Recently, graphene and graphene oxide are a nanomaterial which have been tested for wastewater treatment. Graphene oxide (GO) has been widely studied as a promising photo-absorbing agent for photothermal therapy (PTT) due to its high photothermal responsiveness, low toxicity, and low cost [24-26]. Also, the ultrahigh surface area of graphene oxide (GO) and its polyaromatic structures, represent as efficient for loading the aromatic hydrophobic drugs via hydrophobic interaction and π-π stacking [27-29]. Reduced GO (nrGO), due to the considerably enhanced optical absorbance and the highly restored conjugated structures, is more efficient in PTT.

Chemical reduction of graphene oxide (GO) to graphene require the use of harmful chemicals and toxic environmentally reducing agents, restrict the mass production of reduced graphene which is of tremendous technological importance. In our work we report a green approach to the production of graphene, using bio-reduced by crude glucose. The polysaccharide reduces graphene oxide (GO) to reduced graphene at room temperature in an aqueous medium. Because of the

accessibility, the mild reduction ability, presence of many oxidative groups, and nontoxicity, glucose is considered as an excellent green material for the reduction of GO [30-33]. Zhu et al. [31] in their work used glucose as reductant to reduce GO, the reaction was carried out at 95°C for 60 min in the presence of reducing sugar and ammonia solution in the reaction media. The ammonia solution was used as catalyst to synergistically encourage the reduction reaction and benefit the deoxygenation of GO, and it was shown that such reducing capability related to the ability of the saccharides to form open-chain structures [15]. Chiang et al. [33] also used iron (Fe) as catalyst to accelerate the electron transfer between GO and glucose. Moreover, Yuan et al. [32] in their work, reduced GO using glucose in ammonia solution under 95°C for 2 h to obtain nrGO with high specific surface area and micro- and meso-pore in its structure, Shen and co-works also reduced GO in this solution with different amounts of glucose and ammonia in an autoclave under 160°C for 4 h to obtain rGO with 4.59 of C/O ratio [33-43]. However, these synthetic materials become sediments after centrifugation, thus they are too heavy and unsuitable for loading abundant drugs.

In our work, we tested a novel green route to reduce nano-GO (nrGO) by adopting pure glucose as a reductant to obtain reduced nano-graphene oxide (nrGO). The nrGO obtained was then used for selected pharmaceuticals and personal care products (PPCPs) loading and removal from aqueous solutions under UV light. The studied PPCPs includes: bezafibrate, clofibric acid, carbamazepine, diclofenac. Before to the reduction, nGO was treated by a simple microwave to enable easy nitronium oxidation on graphite oxide. The resulting nrGO has three advantages: (1) excellent biocompatibility: very stable for more than 1 month in water; (2) effective photothermal character: ~10.2-fold increment in NIR absorption at 808 nm compared with the unreduced nGO; and (3) high PPCPs loading ability. Moreover, loaded drugs can be effectively released using acid condition or glutathione (GSH) or heating. These characteristics make the nrGO produced in our work as an excellent nano-composite for high-efficiency in PPCPs loading and removal.

Experimental

Synthesis of nGO

We prepared graphite oxide by a modified Hummer's method using expandable graphite flake. For oxidation process, 15 mg of graphite oxide was mixed with nitronium ion solution in a microwave reaction kettle for 25 s, and then the mixture was put into a microwave reactor chamber to be heated for 10 min at the power of 150 W. After cooling the mixturein ice bath, the reaction mixture was quenched with 100 mL of deionized water, neutralized by NaOH and Na_2CO_3, and ultrafiltered repeatedly through a 30-kDa filter (Millipore) to remove the inorganic salt. Then, the graphite oxide of reoxidation was sonicated at 610 W for 2 h in an ice bath to obtain nGO. The control sample of graphite oxide (nGO-0) was fabricated by sonication of graphite oxide flake at 610 W for 2 h in an ice bath as described by other researchers [19].

Synthesis of nrGO grafted derivative

After 120 mg of glucose was added to 5 mL nGO suspension (about 1 mg/mL) and sonicated for 30 min, the mixture was transferred to autoclave and react at 120°C for 60 min to achieve sterile nrGO. The resulting nrGO was stored at 4°C for further use. The control sample of graphite oxide nrGO-0 was prepared by reducing nGO-0 similarly to the synthesis of nrGO.

Characterization of nrGO

Atomic force microscopy (AFM, Agilent Technologies 5500, USA) was used to image the nrGO on a mica substrate. UV-Vis spectroscopy was performed using a UV-Vis spectrometer (Lambda 35, Perkin-Elmer, Waltham, MA, USA) with a 1-cm quartz cuvette. Absorption spectra were measured using auto microplate reader (Infinite M200, Tecan, Austria). Fourier transform infrared (FTIR) spectra were performed on a FTIR spectrometer (Bruker Tensor 27, Karlsruhe, Germany). Inorder to get nrGO samples without bound glucose for FTIR spectroscopy assay, NaCl was added to nrGO solutions to precipitate nrGO irreversibly, and then the precipitation was centrifuged and rinsed ten times. Raman spectra were performed using Renishaw (New Mills, UK) inVia micro-Raman spectroscopy system equipped with a 514.5-nm Ar^+ laser. Luminescence Spectrometer (LS 55, PerkinElmer, USA) was used to record fluorescence emission of DOX with 488 nm excitation. The images of all samples were done using a digital camera (Nikon, Tokyo, Japan) with 1280 × 1280 pixels resolution. For size distribution measurements, Zeta potential, and polydispersity index (Pdi) of GO materials were conducted with the Zetasizer (Malvern Instruments Ltd., UK), in which mean size=size class (nm) × number distribution date (%).

Adsorption procedure

5 mg of the prepared nrGO absorbents and 50 ml PPCPs solution were put in 50 ml glass bottles and processed in an incubator shaker at a frequency of 100 rpm. The initial concentration of PPCPs is 0-70 mg L^{-1}. The blank experiments without absorbents were also conducted to confirm that the decrease of drug concentration was because of absorbents instead of any other factors. After the adsorption process, the drug concentration was measured by the UV spectrophotometer in phosphate buffer at pH 7.2, at the peak of λ_{max}=273 nm was used for naproxen, λ_{max}=222.4 nm for ibuprofen, λ_{max}=242 nm for oxybenzone, and λ_{max}=254 nm for bezafibrate, λ_{max}=230 nm for clofibric acid, λ_{max}=284.5 nm for carbamazepine and λ_{max}=275 nm for diclofenac. A calibration curve between absorbance and concentration of drug (0-20 mgL^{-1}) was constructed according to the Beer-Lambert's Law. For solutions with concentration higher than 20 mgL^{-1}, the solutions were first diluted with DI water. Meanwhile, kinetic studies were performed at a constant temperature of 25°C and 100 rpm. with 50 mgL^{-1} initial concentration of drug solutions with different adsorption time. The solid-liquid ratio experiments were conducted in 100 mgL^{-1} PPCPs solutions with varying solid-liquid ratio from 1:8 to 1:2. The effect of solution pH on drug removal was studied in the range of 3-10 with 100 mgL^{-1} initial concentrations of PPCPs solutions. The initial pH values of all the solutions were adjusted using 0.1 $molL^{-1}$ HCl or 0.1 $molL^{-1}$ NaOH solution with desired concentrations.

Results and Discussion

Characterization using SEM image

Characterization using SEM image were done to understand the morphological of GO and nrGO, and to test the influence of reduction of nano-GO (nGO) by pure glucose on the change in morphology of the structure. Dozens of SEM images were done for each sample. The typical morphology of SEM pictures of GO and nrGO are presented

in Figures 1A and 1B. SEM images showed GO as wavy, multilayered and folded flakes (Figure 1A). The nrGO images showed that the reduced GO nanocomposite consisted of many layers stacked on top of one another like sheets of paper, with silky, wrinkled and flower-like morphology. The SEM images of GE-nrGO revealed that most of the GO was efficiently reduced to ultrathin sheets with wavy and porous structures of graphene (Figure 1B). The graphene sheets were found to have a curled morphology consisting of a thin, wrinkled, paper-like structure, with approximately four layers and a large specific surface area. This morphology difference observed between the stacked, folded structure of GO and the folded structures of reduced graphene suggests that the GE reduction process played an important role in the transformation of GO to reduced graphene.

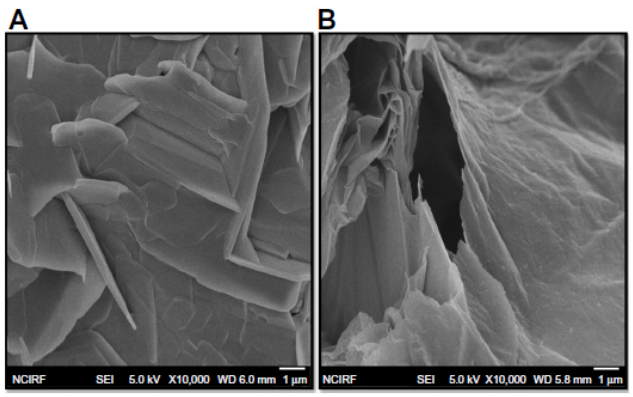

Figure 1: SEM images of (A) GO and (B) nrGO.

Ultraviolet-visible absorption spectra of GO and r-GO

Figure 2 shows ultraviolet-visible absorption spectra of graphene oxide (GO), r-GO and r-GO loading drug after 24 h suspension in water drug solution. The GO spectrum shows an absorbance peak centered at 229 nm, which can be attributed to π-π^* transition of C-C bonds and a prominent shoulder peak at 302 nm, which can be correspond to n-π^* transition of C=O bonds, respectively. The observed r-GO spectrum after reoxidation process for a period of 12 h and 24 h is shown in Figure 1. Upon exposure to oxidizing agent, the peak attributed to π-π^* transition of C-C bonds is red shifted to 263 nm and the shoulder peak at 302 nm is completely disappeared, which indicates the restoration of sp^2 carbon structure. The clear shoulder at 302 nm is started diminishing in less than 1 h of exposure to reducing agent and completely vanished after 2 h. After drug loading the absorption peaks of nGO had a blue shift from 229 nm (nGO-0) to 224 nm due to the destruction of the conjugated structure upon drug interaction. Moreover, the increase in visible light absorption of nGO indicated an exfoliation of graphite oxide during microwave heating and nitronium oxidation. The nrGO has more than a 10.0-fold increase in absorption at 808 nm wavelength over the unreduced nGO. Chen et al. [23] have showed that when reacted with graphite, NO^{2+}can attack the defect-free graphene planes and etch the existing oxidized sites. On the other hand, it was revealed on our work during nitronium oxidation on graphite, multiple hydroxy or epoxy groups were formed. These groups across the surface of the achieved graphene, and subsequent oxidation resulted in more hydroxy and epoxy groups which were preferentially formed away from the carbon atoms already oxidized due to the electron-donating capability of the resulting hydroxy and epoxy groups. These results are consistent with the work of Chen et al. [23]. Thus, we predict that when attacked by NO^{2+}, the GO was covered with a set of elementary oxidation groups, such as hydroxy or epoxy groups, making GO more exposed to the reduction conducted by aldehyde groups from glucose molecules.

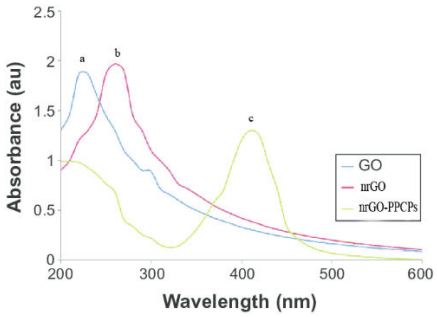

Figure 2: Ultraviolet-visible absorption spectra of (a) graphene oxide (GO), (b) nrGO and (c) nrGO loading PPCPs after 24 h suspension in water drug solution.

XRD analyses of GO and nrGO

The nanocomposite structures of GO and nrGO were tested and confirmed using XRD analysis. Figure 3 shows XRD pattern of (A) GO and (B) nrGO. The XRD results are related to the reduction of GO by glucose and the process of removing the inclusion of water molecules and oxide groups. Three experiments were performed at least for each sample and reproducible results were obtained. The observed characteristic peak of GO at 2θ=11.8 nm, attributed to a d-spacing of 0.74 nm due to the formation of hydroxyl and epoxy and carboxyl groups. However, for the nrGO showed no peaks at 11.8°, seemed to be suggesting that most of the oxygen functional groups of GO were removed, while the presence of an intense diffraction peak at around 26.5° suggesting that the typical π stacking of the GO was functionalized by GE. Thes results also indicates that the glucose played an essential role in deoxygenation of GO. The observed interlayer spacing high value of exfoliated GO was attributed to the introduction of numerous oxygenated functional groups on the carbon sheets. After the exfoliated GO was reduced by GE, a new observed diffraction peak was observed at 2θ=26.5°; with d-spacing=0.35 nm. The noticeable new sharp peak at 2θ=26.5° suggesting a highly organized crystal structure with an interlayer spacing of 0.35 nm. The commercial graphene oxide shows a stacking nanostructure of about 22 × 6 nm average diameter by height with the distance of 0.9 nm between 6-7 graphene layers, whereas the respective reduced graphene oxide (r-GO) about 8 × 1 nm average diameter by height stacking nanostructure with the distance of 0.4 nm between 2-3 graphene layers. All tested graphene oxide samples give the C/O ratio of 2.1-2.3, 26.5-32.1 at% of C sp^3 bonds and high content value of oxygen functional groups (hydroxyl-C-OH, carbonyl-C=Opoxy-C-O-C, carboxyl-C-OOH, water H_2O). Indeed, the reduction process increases the C/O ratio to 2.8-10.3 and decreases C sp^3 content to 11.4-20.3 at% and also the content of C-O-C and C=O groups, go along with increasing content of C-OH and C-OOH groups. The accompanied formation of additional amount of water due to functional oxygen group reduction leads to layer delamination. Removing of functional oxygen groups results in decreasing the distance between the graphene layers.

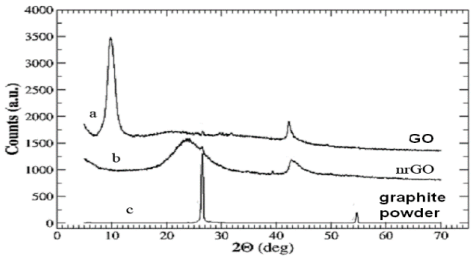

Figure 3: In the XRD pattern of (a) GO, (b) nrGO and (c) graphite powder.

FTIR spectra of GO and nrGO

ATR-IR spectrum in Figure 4 shows a broad band of 3338 cm^{-1}, which is due to O-H stretching vibrations. GO shows peak centered at 1033 cm^{-1} (epoxy or alkoxy C-O), 1154 cm^{-1} (carboxyl C-OH), 1400 cm^{-1} (carboxyl C-O), 1635 cm^{-1} (aromatic C=C), 1716 cm^{-1} (C=O of carboxylic acid). Upon reduction of GO, most of the peaks attributed to oxygen functional groups are disappeared. Even the peaks intensity of carboxyl group at 1400 cm^{-1} is reduced significantly after 2 h of reduction (Figure 4).

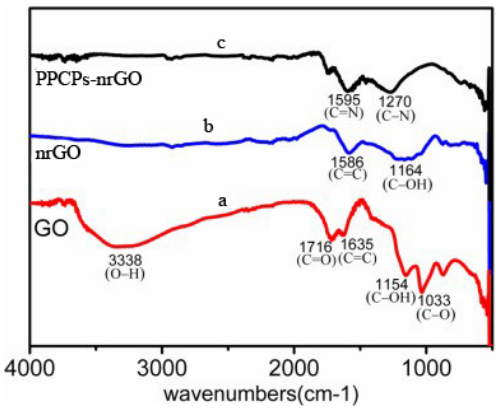

Figure 4: Shows FTIR spectra of the (a) GO, (b) nrGO and (c) PPCPs loading nrGO.

The reduced sample shows interestingly, some new peaks appeared in the spectra, the two prominent peaks centered at 1586 cm^{-1} and 1164 cm^{-1}, attributed to the skeletal vibration of the graphene sheets and are due to the aromatic C=C and C-O stretching. Noteworthy, most of the peaks related to the oxygen-containing functional groups were removed in the FTIR spectrum of r-GO, suggesting that these oxygen-containing functional groups were removed in the process of reduction using glucose. Moreover, as shown in Figure 4, GO had very strong peaks at 3,338 cm^{-1} (O-H), the bands associated with the oxygen functional groups were significantly decreased in nrGO spectra.

The greatly reduced peak at about 1400 and 3338 cm^{-1} of nrGO indicated the removal of the epoxy group and hydroxy (Figure 4). In addition, after drug loading the presence of the peaks at ~ 2920 and ~ 2850 cm^{-1} corresponding to the symmetric and antisymmetric stretching vibrations of the CH2 group and the enhancement of the peaks at ~ 1595 cm^{-1} and ~ 1270 cm^{-1} corresponding to the C=N and C-N stretching vibration, respectively demonstrated that a part of the drug was covalently connected onto the surface of nrGO (Figure 2c).

X-ray photoelectron spectroscopy (XPS) analysis of GO and nrGO

X-ray photoelectron spectroscopy (XPS) is an indispensible technique for elucidating the empirical formula, the elemental composition, chemical and electronic state of substances. In our work it was used to investigate the chemical analysis of GO and nrGO. The calculated binding energy of 285.0 eV was assigned for the C-C, C=C, and C-H bonds on the surface of GO sheets. Furthermore, the observed large peaks at 284.6 eV in Figure 5A corresponding to sp^2 carbon components, and the large oxygenated carbon-related signals peaks at 286-289 eV attributed to C-O single-bond components of hydroxyl and epoxide. These peaks which corresponding to epoxide and hydroxyl groups were significantly decreased after reduction by glucose, thus suggesting that most of the epoxide, hydroxyl, and carboxyl functional groups were removed after the reduction. Our results showed that GO exposure to glucose from 1 to 2 hours cause decreased by 60% of oxygen-containing functional groups, indicating a relative chemical reduction of the sheets by interaction with the glucose.

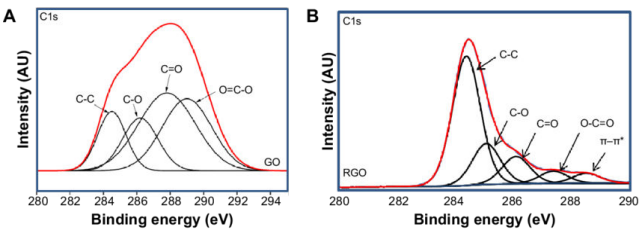

Figure 5: X-ray photoelectron spectroscopy analysis of of C1s in (a) GO and (b) nrGO.

Raman spectra of GO and nrGO

Raman spectroscopy is an important, nondestructive and valuable technique which characterize the structure and quality of carbon materials in the crystal structures. The Raman spectrum of the GO showed a strong G-band at 1,608 cm^{-1} and a D-band at 1,355 cm^{-1} as seen in Figure 6A. The G-band is designated for E2 g phonon of C sp^2 atoms, and the D-band is designated for breathing mode of κ-point phonons of A1g symmetry. Figure 6B display the Raman spectrum of nrGO, it is clear that the G-band was broadened and shifted upward to 1,587 cm^{-1}. However, the intensity of the D-band showed at 1,351 cm^{-1} was increased substantially. These changes could be attributed to the significant decrease of the size of the in-plane sp^2 domains due to oxidation and ultrasonic exfoliation and the partially ordered of crystal structure of reduced graphene nanosheets. The obtained data from Raman spectra of nrGO give evidence for a structural change due to the reduction process by glucose. The observed G-peak and D-peak were both widened and were shifted to approximately to 1,587 cm^{-1} and 1,351 cm^{-1}, respectively (Figures 6A and 6B). Interestingly, the D/G intensity ratio of nrGO (2.1) was higher than that of GO (1.8), suggesting the introduction of sp^3 defects after functionalization and incomplete recovery of the structure of graphene. However, the

increase in the D/G intensity ratio, indicating a decrease in the size of the in-plane sp^2 domains and a partially ordered crystal structure of the r-GO. The noticed variations in the relative intensities of the G-peak and D- peak indicate a change in the electronic conjugation state. These changes suggesting an increase in the number of sp2 domains following reduction of GO. Raman spectra of drug-nrGO samples give evidence for a structural change during drug complexation porcess. The G-peak and D-peak were both widened, the G-peak were shifted further to 1,598 cm^{-1}, 1,595 cm^{-1}. In addition, the D-peak were shifted further to 1,335 cm^{-1}, 1,337 cm^{-1} respectively (Figures 6C and 6D). Interestingly, the G-peak and D-peak were both split indicating sp^3 defects after complexation with the drugs. However, the observed increase in the G/D intensity ratio, suggests an increase in the size of the in-plane sp^2 domains and a partially disordered crystal structure of the drug- rGO complex. Thus, the variations in the relative intensities of the G-peak and D- peak indicate covalent interaction between the drug and the nrGO, a change in the electronic conjugation state of the graphine.

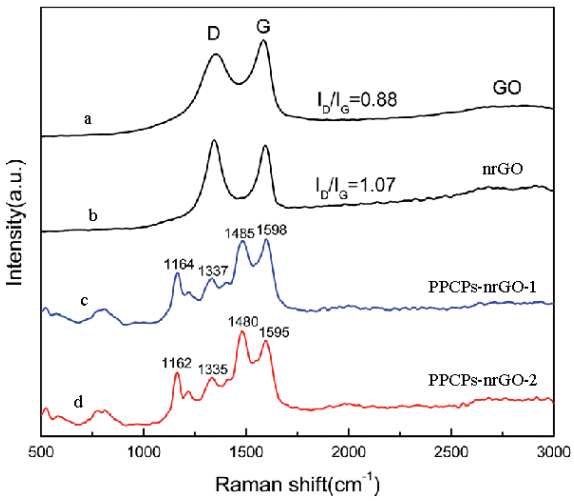

Figure 6: Raman spectroscopy analyses of (a) GO (b) nrGO and (c) PPCPs-nrGO sample-1 and (d) PPCPs - nrGO sample-2.

Atomic force microscopy characterization of GO and nrGO

Atomic force microscopy (AFM) is a topographic technique wih three-dimensional and high atomic resolution to measure surface roughness. The technique was applied to further measure the height and surface profiles of GO and nrGO. Figures 7A and 7B show typical AFM images of GO and nrGO, the mean thickness of GO measured to be about 32.58 nm. However, the prepared nrGO was measured to be about 45.97 nm. Thus, our findings suggest that the reducing properties of glucose could account for the observed increase in thickness of nrGO through removal of oxygen-containing functional groups in GO, and the displacement of the sp^3 hybridized carbon atoms slightly above and below the original graphene plane. Which was corresponding to the capping reagent's important role in increasing the thickness of nrGO. Drug-reduced GO nanocomposite showed greater thickness than nrGO, which was attributed to the adhesion forces and adsorption of drug entities on the nrGO surface.

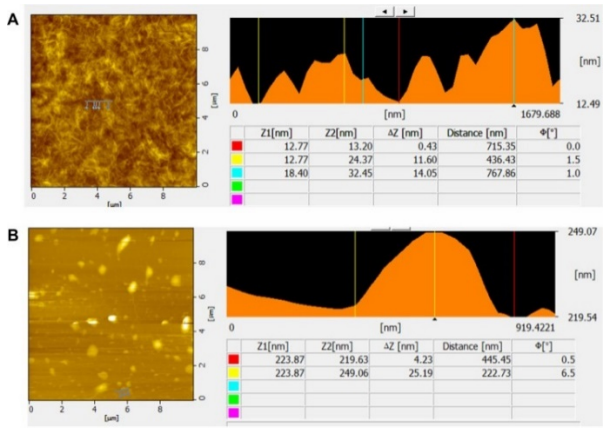

Figure 7: Surface and thickness analysis by atomic force microscopy images of (A) graphene oxide (GO) and (B) Reduced graphene oxide (nrGO).

100 µg of nrGO, indicating the saturated adsorption of DOX on nrGO being at 3.2-folds of weight ratio.

The PPCPs adsorption capacity

The pharmaceuticals and personal care products (PPCPs) accumulation and removal capacity was evaluated by placing the as-prepared glucose-reduced nano-graphene oxide (nrGO) nanocomposites in PPCPs aqueous solutions at pH 7.2 and under UV light. The studied PPCPs include: naproxen, ibuprofen and oxybenzone, bezafibrate, clofibric acid, carbamazepine, diclofenac. The nrGO has the probability to act as a light photocatalyst for degradation of drugs in the adsorption process. So, the present adsorption experiments were measured and repeated in almost dark condition. The concentration of the PPCPs was determined at λ_{max} for each one. The absorption maxima were measured at λ_{max}=273 nm for naproxen, λ_{max}=222.4 nm for ibuprofen, λ_{max}=242 nm for oxybenzone, λ_{max}=254 nm for bezafibrate, λ_{max}=230 nm for clofibric acid, λ_{max}=284.5 nm for carbamazepine and λ_{max}=275 nm for diclofenac. A calibration curve between absorbance and concentration of drug (0 - 20 mgL^{-1}) was constructed according to the Beer-Lambert's Law. For solutions with concentration higher than 20 mgL^{-1}, the solutions were first diluted with DI water. In order to determine the concentration of drugs residual form wastewater samples, samples were collected at different time intervals. The drugs removal rates were calculated according to the equation of K=(A0-AT)/A0 × 100%, where K is the PPCPs removal rate, A0 is the absorbance of the drug stock solution, and AT is the absorbance of the supernatant liquid collected at different time intervals. Table 1 shows the percent of PPCPs removal under visible and UV light, respectively. Under UV illumination diclofenac, naproxen and carbamazepine was almost completely degraded. The percent of drug removal using nrGO nanocomposites can reach nearly 100% for diclofenac, naproxen and carbamazepine under UV light and 91% under visible light. Naproxen and carbamazepine removal using nrGO nanocomposites 95% and 93% were removed under UV light 83% and 86% were removed under visible light, respectively. For bezafibrate, ibuprofen and oxybenzone removal using nrGO nanocomposites 90%, 89% and 86% were removed under UV light 89%, 82% and 80% were removed under visible light, respectively

Whereas for Clofibric acid nearly 60% were removed under UV light and 52% under visible light. Thus, glucose-reduced nano-graphene oxide (nrGO) nanocomposites offer a green alternative to synthetic polymers in the preparation of soft nanomaterials for removal of PPCPs in wastewater.

The adsorption capacity of diclofenac, naproxen and carbamazepine to nrGO nanocomposite was the highest (approx. 500.0 mgg^{-1}, 493.4 mgg^{-1}, 490.5 mgg^{-1}). The calculated maximum adsorption capacities of bezafibrate, ibuprofen, oxybenzone and Clofibric acid under UV light were 325.5, 348.2, 315.8, and 245.3 mg/g, respectively).

PPCPs	Results[a] ± S.D. Using nrGO under visible light	Results[a] ± S.D. Using nrGO under UV light
diclofenac	91%	99%
Naproxen	83%	95%
carbamazepine	86%	93%
bezafibrate	89%	90%
ibuprofen	82%	89%
oxybenzone	80%	86%
Clofibric acid	52%	60%
a: Mean of three determinations		

Table 1: The compared remedation of PPCPs pollutants from wastewater with nrGO nanocomposites under visible and UV light.

Conclusions

Based on our results, nrGO nanocomposite can be used for accumulation and removal of pharmaceuticals and personal care products (PPCPs) from wastewater. The PPCPs can form inner-sphere complexes with the surfaces of nrGO nanocomposite. The adsorption kinetics studies show that the kinetics data conform to the pseudo-second-order kinetics model. The maximum adsorption capacity for diclofenac is 500.0 mgg^{-1}, naproxen is 493.4 mgg^{-1} and carbamazepine is 490.5 mgg^{-1}. The calculated maximum adsorption capacities of bezafibrate is 325.5 mgg^{-1}, ibuprofen is 348.2 mgg^{-1}, oxybenzone is 315.8 mgg^{-1} and Clofibric acid is 245.3 mgg^{-1}. High adsorption capacity was observed even after 4 cycles of adsorption tests, indicating that it has an excellent regeneration performance. The adsorption ability is based on hydrogen bonding or ion interactions with PPCPs as well as π-π interactions of nrGO nanocomposite with aromatic rings of drugs. Finally, the major conclusion of this work is the existence of a huge amount of literature regarding these types of graphene-based nanocomposites and the opportunity existing to further expand graphene chemistry in order to synthesize more stable and effective materials with improved properties for innovative applications.

Conflicts of Interest

The authors declare no conflict of interest regarding the publication of this paper.

References

1. Bulloch DN, Nelson ED, Carr SA, Wissman CR, Armstrong JL, et al. (2015) Occurrence of Halogenated Transformation Products of Selected Pharmaceuticals and Personal Care Products in Secondary and Tertiary Treated Wastewaters from Southern California. Environ Sci Technol 49: 2044-2051.
2. Bu Q, Wang B, Huang J, Deng S, Yu G (2013) Pharmaceuticals and personal care products in the aquatic environment in China: A review. J Hazard Mater 262: 189-211.
3. Jung C, Her NG, Zoh KD, Cho J, Yoon Y, et al. (2015) Removal of endocrine disrupting compounds, pharmaceuticals, and personal care products in water using carbon nanotubes: A review. J Ind Eng Chem 27: 1-11.
4. Dong S, Feng J, Fan M, Pi Y, Hu L, et al. (2015) Recent developments in heterogeneous photocatalytic water treatment using visible light-responsive photocatalysts: a review. RSC Adv 5: 14610-14630.
5. Richardson SD, Ternes TA (2014) Water Analysis: Emerging Contaminants and Current Issues. Anal Chem 86: 2813-2848.
6. Gadipelly C, González AP, Yadav GD, Ortiz I, Ibáñez R, et al. (2014) Pharmaceutical Industry Wastewater: Review of the Technologies for Water Treatment and Reuse. Ind Eng Chem Res 53: 11571-11592
7. Wu X, Conkle JL, Ernst F, Gan J (2014) Treated Wastewater Irrigation: Uptake of Pharmaceutical and Personal Care Products by Common Vegetables under Field Conditions. Environ Sci Technol 48: 11286-11293.
8. Miller EL, Nason SL, Karthikeyan KG, Pedersen JA (2016) Root Uptake of Pharmaceutical and Personal Care Product Ingredients. Environ Sci Technol 50: 525-541.
9. Tanoue R, Nomiyama K, Nakamura H, Kim JW, Isobe T, et al. (2015) Uptake and Tissue Distribution of Pharmaceuticals and Personal Care Products in Wild Fish from Treated-Wastewater-Impacted Streams. Environ Sci Technol 49: 11649-11658.
10. Subedi B, Du B, Chambliss CK, Koschorreck J, Rüdel H, et al. (2012) Occurrence of pharmaceuticals and personal care products in German fish tissue: A national study. Environ Sci Technol 46: 9047-9054.
11. Jiménez SR, González MMM, Maldonado AJH (2010) Metal (M = Co2+, Ni2+ and Cu2+) grafted mesoporous SBA-15: Effect of transition metal incorporation and pH conditions on the adsorption of Naproxen from water. Microporous Mesoporous Materials 132: 470-479.
12. Rivera J, Sindia M, Hernández M, Arturo J (2008) Nickel (II) grafted MCM-41: A novel sorbent for the removal of naproxen from water. Microporous Mesoporous Mater 116: 246-252.
13. Esplugas S, Bila DM, Krause LG, Dezotti M (2007) Ozonation and advanced oxidation technologies to remove endocrine disrupting chemicals (EDCs) and pharmaceuticals and personal care products (PPCPs) in water effluents. J Hazard Mater 149: 631-642.
14. Maria K, Dionissios M, Despo K (2009) Removal of residual pharmaceuticals from aqueous systems by advanced oxidation processes. Env Int 35: 402-417.
15. Yang K, Zhang S, Zhang GX, Sun XM, Lee ST, et al. (2010) Graphene in mice: ultrahigh in vivo tumor uptake and efficient photothermal therapy. Nano Lett 10: 3318-3323.
16. Markovic ZM, Harhaji-Trajkovic LM, Todorovic-Markovic BM, Kepic DP, Arsikin KM, et al. (2011) In vitro comparison of the photothermal anticancer activity of graphene nanoparticles and carbon nanotubes. Biomaterials 32: 1121-1129.
17. Feng L, Wu L, Qu X (2013) New Horizons for Diagnostics and Therapeutic Applications of Graphene and Graphene Oxide. Adv Mater 25: 168-186.
18. Liu Z, Robinson JT, Sun XM, Dai HJ (2008) PEGylated nanographene oxide for delivery of water-insoluble cancer drugs. J Am Chem Soc 130: 10876-10877.
19. Zhang LM, Xia JG, Zhao QH, Liu LW, Zhang ZJ (2010) Functional graphene oxide as a nanocarrier for controlled loading and targeted delivery of mixed anticancer drugs. Small 6: 537-544.

20. Jiang TY, Sun WJ, Zhu QW, Burns NA, Khan SA, et al. (2014) Furin-mediated sequential delivery of anticancer cytokine and small-molecule drug shuttled by graphene. Adv Mater 27: 1021-1028.
21. Robinson JT, Tabakman SM, Liang YY, Wang HL, Casalongue HS, et al. (2011) Ultra small reduced graphene oxide with high near-infrared absorbance for photothermal therapy. J Am Chem Soc 133: 6825-6831.
22. Sheng ZH, Song L, Zheng JX, Hu DH, He M, et al. (2013) Protein-assisted fabrication of nano-reduced graphene oxide for combined in vivo photoacoustic imaging and photothermal therapy. Biomaterials 34: 5236-5243.
23. Chen JQ, Wang XP, Chen TS (2014) Facile and green reduction of covalently PEGylated nanographene oxide via a 'water-only' route for high-efficiency photothermal therapy. Nanoscale Res Lett 9: 86-96.
24. Chen JQ, Liu HY, Zhao CB, Qin GQ, Xi GN, et al. (2014) One-step reduction and PEGylation of graphene oxide for photothermally controlled drug delivery. Biomaterials 35: 4986-4995.
25. Zhu CZ, Guo SJ, Fang YX, Dong SJ (2010) Reducing sugar: New functional molecules for the green synthesis of graphene nanosheets. ACS Nano 4: 2429-2437.
26. Yuan WH, Li BQ, Li L (2011) A green synthetic approach to graphene nanosheets for hydrogen adsorption. Appl Surf Sci 257: 10183-10187.
27. Shen JF, Yan B, Shi M, Ma HW, Li N, et al. (2011) One step hydrothermal synthesis of TiO2-reduced graphene oxide sheets. J Mater Chem 21: 3415-3421.
28. Akhavan O, Ghaderi E, Aghayee S, Fereydoonia Y, Talebi A (2012) The use of a glucose-reduced graphene oxide suspension for photothermal cancer therapy. J Mater Chem 22: 13773-13781.
29. Chua CK, Pumera M (2014) Chemical reduction of graphene oxide: a synthetic chemistry viewpoint. Chem Soc Rev 43: 291-312.
30. Hummers WS, Offeman RE (1958) Preparation of graphitic oxide. J Am Chem Soc 80: 1339-1339.
31. Kovtyukhova NI, Ollivier PJ, Martin BR, Mallouk TE, Chizhik SA, et al. (1999) Layer-by-layer assembly of ultrathin composite films from micron-sized graphite oxide sheets and polycations. Chem Mater 11: 771-778.
32. Blackstock DJ, Gretney JR, Fischer A, Hartshorn MP, Richards KE, et al. (1970) Isomeric diene intermadiates and an acetate rearrangement in aromatic acetoxylation. Tetrahedron Lett 11: 2793-2796.
33. Forsman WC, Mertwoy HE (1980) Intercalation of graphite by nitronium ion attack. Synthetic Met 2: 171-176.
34. Chiang LY, Upasani RB, Swirczewski JW (1992) Versatile nitronium chemistry for C60 fullerene functionalization. J Am Chem Soc 114: 10154-10157.
35. Patel MA, Yang H, Chiu PL, Mastrogiovanni DDT, Flach CR, et al. (2013) Direct production of graphene nanosheets for near infrared photoacoustic imaging. ACS Nano 7: 8147-8157.
36. Edwards HGM, Turner JMC, Fawcett V (1995) Raman spectroscopic study of nitronium Ion formation in mixtures of nitric acid, sulfuric acid and water. J Chem Soc Faraday Trans 91: 1439-1443.
37. Wei T, Fan ZJ, Luo GL, Zheng C, Xie DS (2008) A rapid and efficient method to prepare exfoliated graphite by microwave irradiation. Carbon 47: 337-339.
38. Chen WF, Yan LF, Bangal PR (2010) Preparation of graphene by the rapid and mild thermal reduction of graphene oxide induced by microwaves. Carbon 48: 1146-1152.
39. Zhu YW, Murali S, Stoller MD, Velamakanni A, Piner RD, et al. (2010) Microwave assisted exfoliation and reduction of graphite oxide for ultracapacitors. Carbon 48: 2118-2122.
40. Esteves PM, Carneiro JWD, Cardoso SP, Barbosa AGH, Laali KK, et al. (2003) Unified mechanistic concept of electrophilic aromatic nitration: convergence of computational results and experimental data. J Am Chem Soc 125: 4836-4849.
41. de Queiroz JF, Carneiro JWD, Sabino AA, Sparrapan R, Eberlin MN, et al. (2006) Electrophilic aromatic nitration: understanding its mechanism and substituent effects. J Org Chem 71: 6192-6203.
42. Chiu PL, Mastrogiovanni DDT, Wei DG, Louis C, Jeong M, et al. (2012) Microwave- and nitronium ion-enabled rapid and direct production of highly conductive low-oxygen graphene. J Am Chem Soc 134: 5850-5856.
43. Bose S, Kuila T, Mishra AK, Kim NH, Lee JH (2012) Dual role of glycine as a chemical functionalizer and a reducing agent in the preparation of graphene: an environmentally friendly method. J Mater Chem 22: 9696-9703.